

AD-A063 013

AIR FORCE GEOPHYSICS LAB HANSCOM AFB MASS
A COMPARISON OF THEORETICAL AND EXPERIMENTAL RESULTS IN SUPERCO--ETC(U)
AUG 78 R M DYER, B A KUNKEL
AFGL-TR-78-0103

F/G 4/1

UNCLASSIFIED

NL

[OF]
AD
A063013



END
DATE
FILMED
3--79
DDC

DDC FILE COPY AD A063013

LEVEL II

12

14

AFGL-TR-78-0193

AIR FORCE SURVEYS IN GEOPHYSICS

AFGL-AFSG-395



6

A Comparison of Theoretical and Experimental Results in Supercooled Stratus Dispersal

10

ROSEMARY M. DYER
BRUCE A. KUNKEL

9

Air Force surveys in geophysics,

DDC
RECEIVED
9 JAN 1979
E

11

9 Aug 1978

12

21p.

Approved for public release; distribution unlimited.

16

667p

17

11

METEOROLOGY DIVISION PROJECT 6670
AIR FORCE GEOPHYSICS LABORATORY
HANSCOM AFB, MASSACHUSETTS 01731

AIR FORCE SYSTEMS COMMAND, USAF



409 578

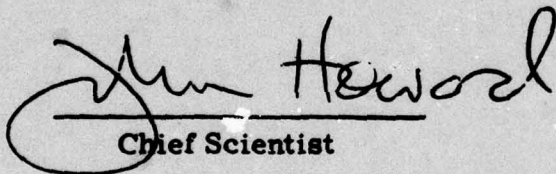
79 01 08 020

mt

This report has been reviewed by the ESD Information Office (OI) and is releasable to the National Technical Information Service (NTIS).

This technical report has been reviewed and is approved for publication.

FOR THE COMMANDER


Chief Scientist

Qualified requestors may obtain additional copies from the Defense Documentation Center. All others should apply to the National Technical Information Service.

Printed by
United States Air Force
Hanscom AFB, Mass. 01731

Unclassified

SECURITY CLASSIFICATION OF THIS PAGE (When Data Entered)

REPORT DOCUMENTATION PAGE		READ INSTRUCTIONS BEFORE COMPLETING FORM
1. REPORT NUMBER AFGL-TR-78-0193 ✓	2. GOVT ACCESSION NO.	3. RECIPIENT'S CATALOG NUMBER
4. TITLE (and Subtitle) A COMPARISON OF THEORETICAL AND EXPERIMENTAL RESULTS IN SUPERCOOLED STRATUS DISPERSAL	5. TYPE OF REPORT & PERIOD COVERED Scientific. Interim.	
	6. PERFORMING ORG. REPORT NUMBER AFSG No. 395 ✓	
7. AUTHOR(s) Rosemary M. Dyer Bruce A. Kunkel	8. CONTRACT OR GRANT NUMBER(s)	
9. PERFORMING ORGANIZATION NAME AND ADDRESS Air Force Geophysics Laboratory (LYP) Hanscom AFB Massachusetts 01731	10. PROGRAM ELEMENT, PROJECT, TASK AREA & WORK UNIT NUMBERS 62101F 66701101	
11. CONTROLLING OFFICE NAME AND ADDRESS Air Force Geophysics Laboratory (LYP) Hanscom AFB Massachusetts 01731	12. REPORT DATE 9 August 1978	
	13. NUMBER OF PAGES 19	
14. MONITORING AGENCY NAME & ADDRESS (if different from Controlling Office)	15. SECURITY CLASS. (of this report) Unclassified	
	15a. DECLASSIFICATION/DOWNGRADING SCHEDULE	
16. DISTRIBUTION STATEMENT (of this Report) Approved for public release; distribution unlimited.		
17. DISTRIBUTION STATEMENT (of the abstract entered in Block 20, if different from Report)		
18. SUPPLEMENTARY NOTES		
19. KEY WORDS (Continue on reverse side if necessary and identify by block number) Stratus dispersal Supercooled stratus Cloud models Cloud seeding		
20. ABSTRACT (Continue on reverse side if necessary and identify by block number) ▶ A one-dimensional mathematical model of the growth of ice crystals in supercooled clouds was examined in detail and a sensitivity analysis was performed. Critical parameters include seeding rate, temperature, cloud depth, liquid water content, drop size, and updraft velocities. Calculations were compared with experimental observations made during a stratus seeding field program conducted in Northern Michigan in 1977. Substituting reasonable values of cloud physics parameters and using known values of the seeding rates, minimum temperatures, and cloud depth, reasonable agreement between		

DD FORM 1 JAN 73 1473

EDITION OF 1 NOV 65 IS OBSOLETE

Unclassified

SECURITY CLASSIFICATION OF THIS PAGE (When Data Entered)

79 01 08 020

Unclassified

SECURITY CLASSIFICATION OF THIS PAGE(When Data Entered)

20. (Cont)

theoretical and observed rates of cloud dissipation was obtained.

A

Unclassified

SECURITY CLASSIFICATION OF THIS PAGE(When Data Entered)

ACCESSION for	
NTIS	White Section <input checked="" type="checkbox"/>
DDC	Buff Section <input type="checkbox"/>
UNANNOUNCED	<input type="checkbox"/>
JUSTIFICATION	
BY	
DISTRIBUTION/AVAILABILITY CODES	
Dist.	SPECIAL
A	

Contents

1. INTRODUCTION	5
2. SENSITIVITY ANALYSIS OF THE MATHEMATICAL MODEL	6
2.1 Seeding Rate	6
2.2 Temperature	7
2.3 Vertical Motions	8
2.4 Liquid Water Content and Cloud Drop Size	9
3. COMPARISON BETWEEN MODEL AND FIELD TESTS	10
4. CONCLUSIONS AND RECOMMENDATIONS	13
APPENDIX A: Mathematical Model of Crystal Growth in Clouds	15

Illustrations

1. Effect of Ice Nuclei Concentration on Clearing Rate	7
2. Effect of Temperature on Clearing Rate	8
3. Effect of Vertical Motion on Clearing Rate	9
4. Effect of Cloud Liquid Water Content and Drop Size on Clearing Rate	9
5. Efficiency of Chlorine-doped Silver Iodide Flares (solid line) and Non-doped Flares (dashed line)	11

Tables

1. Comparison Between Theoretical and Observed Clearing Times

12

A Comparison of Theoretical and Experimental Results in Supercooled Stratus Dispersal

1. INTRODUCTION

The dissipation of supercooled stratus clouds by seeding with dry ice or silver iodide has often been a haphazard procedure. Vickers and Church¹ determined an optimum size and seeding rate for dry ice by applying operations analysis techniques to a series of experiments in thin stratus clouds. However, indiscriminate extrapolation of their results to thicker cloud decks or to silver iodide seeding can produce overseeding of the clouds. At its worst, this prevents clearing, because the ice crystals generated remain suspended in the cloud instead of precipitating out. Even when this does not occur, the efficiency of the silver iodide seeding technique is decreased to the point where the acquired visibilities are not adequate for the desired operation.

Chappell and Smith² derived a one-dimensional mathematical model of the growth of ice crystals in supercooled clouds. The ideal ice concentration is a function of temperature, liquid water content, drop size distribution, vertical motion, and cloud thickness. The amount of seeding material required to obtain this ideal ice crystal concentration depends on the cloud thickness and the efficiency of the seeding material which is, in turn, a function of temperature.

(Received for publication 9 August 1978)

1. Vickers, W.W., and Church, J. (1966) Investigation of optical design for supercooled cloud dispersal equipment and techniques, J. Meteorol. 5(No. 1):105-118.
2. Chappell, C.F., and Smith, D.R. (1976) On the Crystal Concentrations Needed to Dissipate Cold Stratus Clouds, NOAA, Atmospheric Physics and Chemistry Laboratory, Boulder, Colorado (Unpublished report).

It is usually not possible to measure all pertinent cloud parameters prior to seeding and to date there has been no direct verification of the Chappell-Smith model. However, seeding experiments using chlorine-doped silver iodide flares, conducted in Northern Michigan in February 1977, included measurements of cloud depths and temperatures as well as observations of clearing time. In this report, a sensitivity analysis is done with the model to determine the important parameters and how they affect the clearing efficiency. Model calculations are then compared with actual field results.

2. SENSITIVITY ANALYSIS OF THE MATHEMATICAL MODEL

The equations and assumptions entering the Chappell-Smith, one-dimensional time-dependent, microphysical model are described in Appendix A. This appendix is part of an unpublished report submitted by NOAA/APCL to AFGL in response to work done for AFGL under Project Order No. Y7T-807. In this model, ice nuclei of a given concentration are distributed uniformly throughout a cloud with a given temperature, liquid water content, drop concentration, and vertical velocity. The ice crystals then grow by diffusion and accretion until they fall out of the cloud layer. Fall speeds, based on crystal mass and updraft velocity, are calculated in order to determine fallout times. A sensitivity analysis was performed on this model to determine the effect of varying individual parameters. Some of the results derived from this analysis are presented here.

2.1 Seeding Rate

Pioneers in cloud dispersal sometimes had the naive belief that, if they were able to produce a clearing after a long interval, a higher seeding rate would have produced the same clearing more quickly. This would be true if the only governing factor were the rate at which the cloud drops are converted to ice crystals. However, calculations show that the visibility restriction due to ice crystals is greater than that due to the liquid water. Therefore, the crystals must either fall out or evaporate below the cloud base before clearing can take place. The fallout time is directly related to how fast the ice crystals take on water—the fewer the crystals, the less competition for the available water and the faster they will grow and fall out.

This is illustrated in Figure 1. The curves of this figure were obtained by varying the number of ice nuclei per volume of air, keeping all other parameters constant. The time it takes to achieve an arbitrary horizontal visibility of 1.5 km steadily decreases with increasing nuclei concentration. The resulting horizontal visibility will vary with depth because of the differences in the ice crystal residence time. If the seeding material is distributed uniformly over the depth of the cloud,

then residence time decreases with increased height and, therefore, maximum visibility improvement occurs near the base of the cloud.

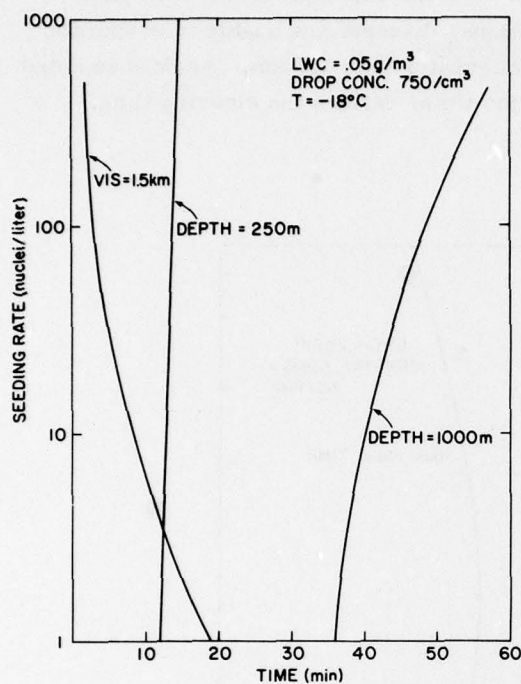


Figure 1. Effect of Ice Nuclei Concentration on Clearing Rate

The time it takes for the resulting ice crystals to fall through the cloud actually increases with increasing seeding rate. As can be seen in Figure 1, increasing the seeding rate will only increase this time. For the thinner cloud (250 m) the seeding rate is not so critical. At seeding rates less than 3 nuclei/liter, the ice nuclei fall out of the thinner cloud before the visibility near the cloud base reaches 1.5 km, thus restricting the visibility improvement to something less than 1.5 km. However, in such shallow cloud layers, the ground can be visible even when the cloud visibility is much less than 1.5 km.

2.2 Seeding Rate

Cloud temperature affects the efficiency of the seeding material (the number of ice nuclei generated per gram of seeding material) and also the rate of diffusion of water vapor to the ice crystals. The model assumes a given concentration of ice nuclei per volume and, therefore, treats only the second effect. The diffusion rate is a function of the difference between the vapor pressure over water and over ice.

Since the greatest difference occurs at approximately -12°C , it would be expected that the faster clearings would occur at this temperature. Figure 2 shows this to be true. However, the differences in clearing time are quite small between -10° and -25°C . At temperatures warmer than -4°C the vapor pressure difference is so small that, at least for the given conditions, droplets are unable to evaporate sufficiently to raise the visibility to a level greater than 1.5 km. Again it is noted that the fallout time, and not the evaporation time, defines the clearing time.

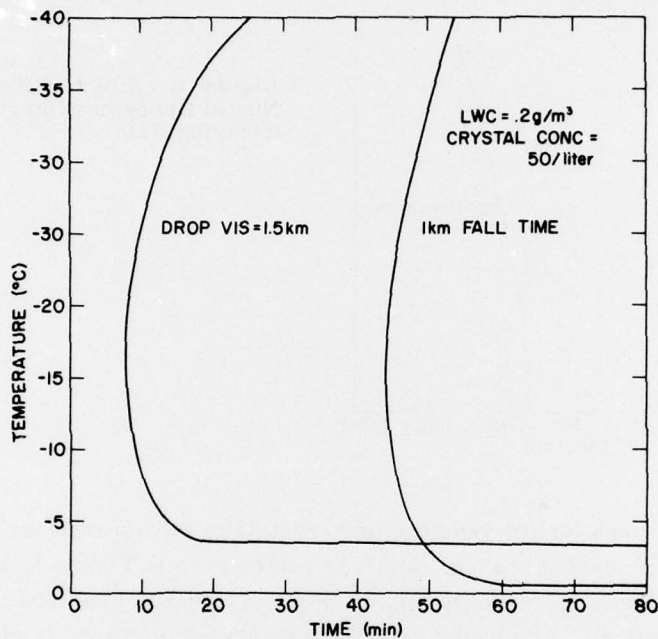


Figure 2. Effect of Temperature on Clearing Rate

2.3 Vertical Motions

Computations at a variety of temperatures, seeding rates, and liquid water contents were made assuming updrafts of up to 10 cm/sec. As expected, the fallout time increases with increasing updraft velocity, thus increasing the time to clear as shown in Figure 3. In this example, the clearing time increases 23 percent (from 44 min to 54 min) when the updraft velocity increases from 0 to 10 cm/sec.

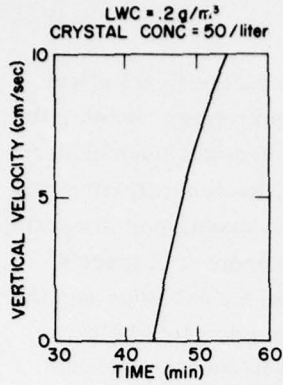


Figure 3. Effect of Vertical Motion on Clearing Rate

2.4 Liquid Water Content and Cloud Drop Size

When computations were made in which the cloud liquid water content (LWC) was varied, the results were as shown in the solid curve of Figure 4—a gradually decreasing time to clear with increasing LWC. In these computations the cloud drop size was held constant, so that increasing LWC also means increasing concentration. The decreasing time with increasing liquid water is due to the fact that the crystals grow larger with increasing liquid water and thus have a greater terminal velocity.

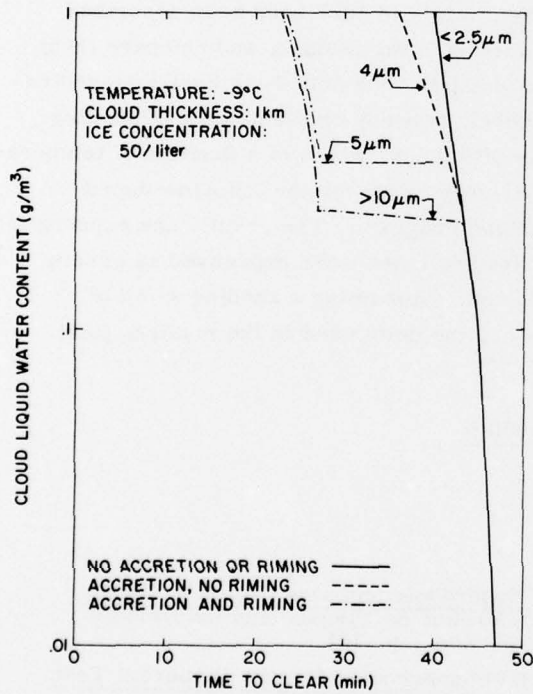


Figure 4. Effect of Cloud Liquid Water Content and Drop Size on Clearing Rate

Assuming no accretion or riming, cloud drop size has an insignificant effect on clearing rate. However, with increasing drop size and liquid water content, the probability of accretion and riming increases. Larger cloud droplets have higher collision efficiencies, and the higher the liquid water content, or concentration, the more likely that collisions and riming will occur. For a given mass, rimed crystals fall faster than unrimed crystals and, therefore, will fall out sooner. Figure 4 shows that riming occurs when cloud droplets are greater than $4 \mu\text{m}$ radius and the liquid water content is greater than about 0.3 g/m^3 . For cloud droplets below $2.5 \mu\text{m}$ radius the model assumes the collection efficiency to be zero. Between 2.5 and $4 \mu\text{m}$, the collection efficiencies are quite low but not zero, thus causing some accretion but not enough to cause riming—at least as defined by the model. The model arbitrarily assumes that riming occurs if the accretion rate is greater than the diffusion rate. No experimental data exist to demonstrate how accurate this assumption is and whether or not the sharp discontinuity shown in Figure 4 actually occurs. In reality, there is probably a gradual transition from unrimed to rimed particles.

3. COMPARISON BETWEEN MODEL AND FIELD TESTS

The tests conducted in northern Michigan early in 1977 have been described elsewhere.^{3,4} In this section we shall summarize the results, and compare them with predictions based on the mathematical model. The actual ice nuclei concentration, which is an input parameter of the model, depends on the amount of seeding material dispensed per unit volume and its efficiency, which is a function of temperature. The solid line in Figure 5 is the efficiency curve for the chlorine-doped silver iodide flares used in the 1977 Michigan program. The results are expressed as nuclei per gram of seeding material. Seeding rates were expressed as grams of AgI per nautical mile per 1000 ft cloud depth. Assuming a seeding width of 1000 m and converting to ice nuclei per liter, the units used in the mathematical model, we obtain

$$\text{nuclei/liter} = \frac{\text{nuclei/nautical mile/1000 ft}}{5.649 \times 10^{11}} \quad (1)$$

3. Dyer, R. M. et al (1977) Dispersal of Supercooled Stratus Clouds by Silver Iodide Seeding, Preprints, Sixth Conference on Planned and Inadvertent Weather Modification, Amer. Meteor. Soc., p. 184.
4. Wisner, C., and Thompson, J.R. (1978) Supercooled Stratus Dispersal Test Program, Final Report, AFGL Contract No. F19628-76-C-0306.

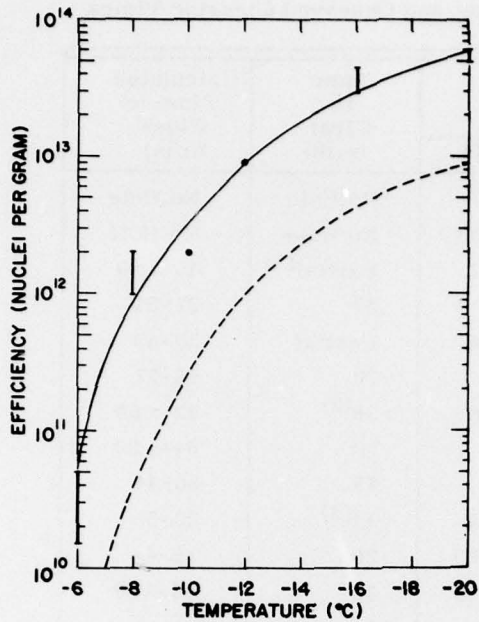


Figure 5. Efficiency of Chlorine-doped Silver Iodide Flares (solid line) and Non-doped Flares (dashed line)

Table 1 summarizes the field results and compares them with the model calculations. The "Observed" parameters are those parameters actually measured during the field tests. Cloud depth was determined from altitude measurements by the aircraft flying at cloud base and at cloud top. The cloud top and cloud base temperatures were obtained from a temperature probe mounted on the aircraft. The seeding rate in terms of g/nautical mile/1000 ft depth is obtained from the number of flares ejected. In the single line tests, as compared with multiple line tests, a variable seeding rate was used. Conversion of this seeding rate to nuclei per liter was done by using the efficiency curve of Figure 5, and the formula of Eq. (1). Time to clear in the "Observed" section is the time at which the observer in the observation plane reported seeing the ground through the stratus deck. The main source of error in this section is the conversion from seeding rate to crystal concentration, depending as it does on a laboratory-measured efficiency curve with some scatter in the measurements. Another source of imprecision is the observed time to clear. The observation aircraft did not always remain atop the seeded area, and on those occasions the clearing would have occurred some minutes before the observation.

Table 1. Comparison Between Theoretical and Observed Clearing Times

Min Temp (°C)	Cloud Depth (m)	Observed Seeding Rate		Time to Clear (min)	Calculated Time to Clear (min)
		(g/nmi/kft)	(No. /l)		
-4	400	20-200	.007-.07	No Hole	No Hole
-6	270	20-200	.638-6.38	No Hole	No Hole
-8.5	1890	30-300	53.1-531	Partial ⁽¹⁾	45->80
-8.5	1070	30	53	39	27-51
-9	1200	10-100	35.4-354	Partial	29-69
-9.5	1370	80	354	70	42-77
-9.5	1200	200	88.6-886	>36 ⁽²⁾	32->80
-10	1310	70	433	70	64->80
-11.5	760	36	383	45	38-44
-12.0	520	7-70	99.2-992	11 ⁽³⁾	29-55
-14.0	460	9-90	287-2870	30	16-44
-15.5	730	8-80	354-3543	38	36->80
-17.5	910	44	2728	38	>80
-17.5	270	30-300	1860-18600	20	20->80
-21.5	488	5-50	708-7086	45	27->80

- (1) 20 g flares were used. This size flare burns over only a 1200 m depth.
 (2) Log does not indicate when ground became visible, but it was sometime after 36 minutes.
 (3) Thin spots were observed in cloud.

The computer model requires values of cloud liquid water content, drop size, and concentration and vertical motion, but these parameters were not measured. Calculations were made using the observed conditions and a variety of assumed liquid water content and drop size conditions. Liquid water content varied from .05 - 0.5 g/m³ and drop diameter from 10.8 - 24 μm. The 0.5 g/m³ liquid water contents represent cases in which riming occurred, and the .05 g/m³ represents cases in which some accretion took place but no riming, according to the model. A cloud drop concentration of 75/cm³ and a zero vertical velocity were assumed. As shown earlier, a change in the drop concentration has little impact on the clearing time except where it means the difference between riming and no riming. Also cases with updrafts will increase the clearing time slightly.

The calculated clearing times show a wide range of possible times. Computations were stopped at 80 min, so the notation > 80 indicates that clearing had not

occurred up to the time computation stopped. In general, the slowest clearing occurs at low liquid water content and high seeding rate. In eight of the eleven cases in which the ground became visible, the observed clearing times were within the calculated range. The model successfully predicted the two cases in which no clearing was observed. Although the seeding rate is relatively high, the number of nuclei produced at these temperatures, as illustrated in Figure 2, is quite low. The model shows the ice crystals falling out before the droplets can evaporate enough to raise the visibility sufficiently to see through the cloud layer.

At the lower temperatures ($< -15^{\circ}\text{C}$) and at the higher seeding rates the model predicts overseeding with ice crystals remaining in suspension rather than precipitating out. This may account for the annulus of unprecipitated ice crystals noted in the center of the seeded area where crystals concentration is highest. It is more likely that the actual ice crystal concentration near the edges of the affected area were considerably less than near the center, thus resulting in more rapid clearing and higher visibilities along the edge. The model, being a one-dimensional model, does not take into account horizontal diffusion and assumes a uniform distribution of ice crystals.

4. CONCLUSIONS AND RECOMMENDATIONS

The field tests have demonstrated the feasibility of silver iodide seeding for tactical dispersal of supercooled stratus clouds, and the one-dimensional mathematical model has provided reasonable estimates of the clearing rate under a variety of meteorological conditions.

Further field tests, including measurements of cloud microphysics, are required to derive a feasible method of determining optimum seeding procedures under operational conditions. A field program using a tactical aircraft would be the ultimate test of whether this technique can become a standard Air Force capability.

The mathematical model needs extension and refinement. Results of field tests during which cloud physics parameters are measured can be used to refine the equations used in the model. Extension of the model to two-dimensions will allow prediction of the ultimate size of the opening, and perhaps how long the visibility remains above minimum. Incorporation of viewing angle into the model would also be desirable, so that slant range visibility may be computed.

Laboratory studies and field tests should also be directed toward determining the optimum composition of the silver iodide flares. The flares used in the Air Force tests in Michigan contained a chlorine compound, which improved their efficiency. The difference between the solid and the dashed curve of Figure 5 is the difference

between the efficiencies of the chlorine-treated and the untreated flares. There are many unanswered questions, such as what proportion of chlorine will optimize the efficiency and what mechanism is operating to produce the ice nuclei from the chlorine-doped silver iodide.

Appendix A

Mathematical Model of Crystal Growth in Clouds

A1. INTRODUCTION

The model derived by Chappell and Smith² has not been described in the open literature. A brief summary of the equations used, taken from Chappell and Smith's internal report to AFGL, is presented here.

A2. LIST OF SYMBOLS

a	Droplet curvature term = $3.3(10^{-5})/T$
b	Droplet solubility term = $1.33925(10^{-15})$
C_p	Specific heat of air at constant pressure
C_v	Specific heat of air at constant volume
D	Diffusivity of water vapor
D_d	Diameter of water droplet
D_p	Diameter of partially rimed crystal
D_u	Diameter of unrimed crystal
e	Vapor pressure of the environment
E	Collection efficiency of crystals for supercooled cloud water
e_i, e_w	Saturation vapor pressure of the environment (over a plane ice surface, over a plane water surface)
g	Gravitational acceleration

G	Thermodynamic function in droplet growth equation
G_i	Thermodynamic function in ice crystal growth equation
K	Thermal conductivity of air or scattering efficiency of a cloud droplet
L_c, L_s	Latent heat of condensation and sublimation
m_c, m_d	Mass of ice crystal and water droplet
N_c, N_d	Concentration of ice crystals and water droplets per unit volume of air
p	Atmospheric pressure
q_{cw}	Cloud liquid water per unit volume
r_d	Radius of water droplet
R_d, R_v	Specific gas constant for dry air, and for water vapor
S_i, S_w	Supersaturation with respect to ice and water
t	Time
T	Temperature
V	Visibility
V_p	Fall velocity of partially rimed ice crystals
V_u	Fall velocity of unrimed ice crystals
W	Updraft velocity
ϵ	Ratio of the molecular weight of water vapor to that of air (0.622)
ρ	Density of air
$\phi_1, \phi_2, \phi_3, \phi_4, \phi_5$	Thermodynamic functions in the supersaturation equation
ψ_1, ψ_2, ψ_3	Thermodynamic functions in the supersaturation equation

A3. CLOUD SUPERSATURATION

Temporal changes in the supersaturation of a mixed-phase cloud are given by

$$\dot{S}_1 = \phi_1 w - \phi_2 (N_d \dot{m}_d + \dot{N}_d m_d) - \phi_3 (N_c \dot{m}_c + \dot{N}_c m_c) - (S_i + 1) (1 - \phi_4 N_d m_d - \phi_5 N_c m_c) (\dot{\rho}/\rho) \quad (A1)$$

where \dot{m}_d and \dot{m}_c are the time rate of changes in droplet and crystal mass, and \dot{N}_d and \dot{N}_c are the time rate of changes in the droplet and crystal concentrations. \dot{N}_c is assumed equal to zero, since agglomeration is not considered. Dots indicate differentiation with respect to time. Eq. (A1) is obtained by combining the Clausius-Clapeyron relation, energy equation, and the equations of state for dry and moist air. It describes changes in cloud supersaturation as a function of the interaction among the updraft, crystal growth, and droplet growth or evaporation.

The thermodynamic functions in Eq. (A1) are given by

$$\phi_1 = \left(\frac{eg\epsilon L_s}{e_i R_d T^2 C_p} - \frac{eg}{e_i R_d T} \right), \quad (A2)$$

$$\phi_2 = \left(\frac{e\epsilon L_s L_c}{e_i p C_p T} + \frac{R_d T}{e_i \epsilon} \right), \quad (A3)$$

$$\phi_3 = \left(\frac{e\epsilon L_s^2}{e_i p C_p T} + \frac{R_d T}{e_i \epsilon} \right), \quad (A4)$$

$$\phi_4 = \left(\frac{\epsilon L_s L_c}{p C_p T} \right), \quad (A5)$$

and

$$\phi_5 = \left(\frac{\epsilon L_s^2}{p C_p T} \right). \quad (A6)$$

The last parenthetical expression in Eq. (A1) is given by

$$\dot{\rho}/\rho = - \frac{[\psi_1 w + \psi_2 (N_d \dot{m}_d + N_d \dot{m}_d) + \psi_3 (N_c \dot{m}_c + N_c \dot{m}_c)]}{1 - \psi_2 N_d \dot{m}_d - \psi_3 N_c \dot{m}_c}, \quad (A7)$$

where the thermodynamic functions are expressed by

$$\psi_1 = \frac{C_v g w}{R_d C_p T}, \quad (A8)$$

$$\psi_2 = \frac{L_c R_d}{C_p p}, \quad (A9)$$

and

$$\psi_3 = \frac{L_s R_d}{C_p p}. \quad (A10)$$

A4. DROPLET GROWTH

Droplet growth in Eq. (A1) is evaluated with the expression

$$\dot{m}_d = 4\pi r_d G \left[S_w - (a/r_d) + (b/r_d^3) \right]. \quad (A11)$$

The Kelvin curvature term is evaluated by $a = 3.3(10^{-5})/T$, and the nucleus solubility term is $b = 1.33925(10^{-15})$. The thermodynamic function is given by

$$G = \left[(L_c^2 / KR_V T^2) + (R_V T / e_w D) \right] . \quad (A12)$$

A5. CRYSTAL GROWTH

For unrimed or slightly rimed crystals, depositional and accretional growth equations are

$$\dot{m}_{cd} = 205.195 m_c^{1/2} S_i G_i (1 + 24.63 m_c^{0.305}) \quad (A13)$$

and

$$\dot{m}_{ca} = 1709.26 E_{q_{cw}} V_u m_c . \quad (A14)$$

where ice crystals are assumed to be planar disks and ventilation effects are included. The thermodynamic function is

$$G_i = \left[(L_s^2 / KR_V T^2) + (R_V T / e_i D) \right]^{-1} , \quad (A15)$$

and the crystal fall velocity is

$$V_u = 62 D_u^{0.217} . \quad (A16)$$

The relationship between crystal size and mass incorporated into Eq. (A13) is

$$m_c = 0.00038 D_u^2 . \quad (A17)$$

The collection efficiency of crystals for supercooled cloud droplets is defined by the function

$$E = 0 \text{ for } D_d < 5\mu \quad (A18)$$

$$E = -0.58576916 + 0.13872401 D_d - 0.0030517645 D_d^2 \text{ for } 5\mu \leq D_d \leq 17.5\mu$$

$$E = 0.91 \text{ for } D_d > 17.5\mu .$$

Crystal growth in Eq. (A1) must include only ice growth by deposition. However, the crystal mass in Eq. (A13) is modified by the accretional growth rate given by Eq. (A14). The time rate of change of droplet concentration due to accretion is then

$$\dot{N}_d = -N_c \dot{m}_{ca} / m_d . \quad (A19)$$

For partially rimed crystals the depositional and accretional growth equations are

$$\dot{m}_{cd} = 96.225 m_c^{1/2} S_i G_i (1 + 28.57 m_c^{0.325}) \quad (A20)$$

and

$$\dot{m}_{ca} = 240.56 E_{cw} V_p m_c . \quad (A21)$$

The crystal fall velocity is given by

$$V_p = 170.7 D_p^{0.3} , \quad (A22)$$

and the relationship between crystal size and mass incorporated into Eq. (A20) is

$$m_c = 0.0027 D_p^2 . \quad (A23)$$

A6. VISIBILITY

Visibility due to the presence of cloud droplets is computed from

$$V = 3.912 / \pi \sum_{i=1}^N (K_i n_i r_{d_i}^2) , \quad (A24)$$

where N is the number concentration of cloud droplets, r_d is the cloud droplet radius, and K is the scattering efficiency of a cloud droplet. The scattering efficiency is taken to have a value of approximately two for visible light and spherical cloud droplets.